
Faculty of Engineering
Nanotechnology Engineering

NE 469: Tactile Sensors

# MFC-based Piezoelectric Finger for Improved Sensitivity in Tissue Stiffness Detection

Prepared by:
Dhilan Bekah (20512356)
Jonathan D. Chan (20517241)
Paulo Miguel (20543044)

April 1, 2018

# Contents

# List of Figures

# List of Tables

# 1 Introduction

## 1.1 Defining the Problem

Among women, breast cancer is the most common form of cancer in the United States and Canada [5, 6]. According to the American Cancer Society, upwards of 260000 women will be diagnosed with breast cancer in 2018, while upwards of 40000 women will die from the disease [7]. Studies have shown that early detection of breast cancer, which then allows for early treatment options, greatly increases the likelihood of survival [8]. Currently, about 32.8% of breast cancer cases are diagnosed at a late stage (when the cancer is no longer localized) [9]. Unlike early stage diagnoses, which have extremely high survival rates, late stage diagnoses have relatively low survival rates after 5 years (72% for stage 3 and 22% for stage 4) [10]. The most critical point for the best prognosis is to identify early stage cancer cells before they get a chance to spread to the local lymph nodes (stage 3) or to other vital organs in the body (stage 4) [11]. This, however, requires a relatively inexpensive and non-invasive test in order for screening to occur regularly.

Currently, mammography is the standard breast cancer screening technique. Although it is a relatively inexpensive screening technique, it's sensitivity is particularly low when trying to identify tumours in women under the age of 40 and women who have dense breasts [12]. Further, mammography is far less sensitive at finding tumours that are less than 1mm in diameter, potentially allowing the cancer to progress to a later stage before it is finally detected [13]. There are other widely used screening techniques, such as ultrasound, MRI, CT, and PET, but each of these techniques have their shortcomings as a primary screening technique [11]. It is therefore imperative that a new technique is found that is both inexpensive and non-invasive, to be used as a primary screening technique for breast tumours.

## 1.2 Challenges

Sensitivity is described as the ratio of positives that were correctly identified as such to those who were not. Selectivity, on the other hand, is described as the ratio of negatives that were correctly identified as such to those who were not [14]. For a primary screening technique, the selectivity of the technique is extremely important (more so than the sensitivity). This is because all positive results could undergo further testing that would give a better understanding the stage and progression of the cancer. False negatives, on the other hand, need to be avoided at all costs. This is because a false negative will not be further tested, thus allowing the cancer to de-

velop until the next round of screening tests occur. Therefore, it is imperative that a primary screening method has a high selectivity (high sensitivity is also important).

Other factors that affect the potential use of a technique as a screening technique are cost, time and how invasive the test is. Millions of women need to be screened for breast cancer on a yearly basis, thus it is imperative that the screening test is inexpensive. This is important for two reasons. First, testing equipment that is very expensive is usually less available and therefore, is unable to accommodate the high volumes of screenings that are required. Second, less expensive tests can be repeated as often as required, thus allowing for better tracking of the screening process over time. Similarly, a non-invasive test that can be done in a short amount of time allow for more tests to be conducted more often. This means that the screening test could be conducted regularly during check ups while not requiring an additional appointment.

Although mammography is currently the gold standard for breast cancer screening, due to its relatively low cost, time and it being non-invasive, it still has a variety of draw backs. The sensitivity of the technique is highly dependent on a variety of attributes including (but not limited to) the age, ethnicity, personal history of the patient, as well as the experience of the radiologist [11]. Mammograms also provide a relatively high number of false-positives and false-negatives, thus proving the technique has low sensitivity and low selectivity. This explains the extremely low decrease in breast cancer death rates of 0.0004% since the technique was introduced [15].

Other commonly used screening techniques follow a similar trend to that of mammography. The majority of common screening tests are either not cost effective, take too long to be scalable to large populations or suffer from poor sensitivity and selectivity ratios. Ultrasounds are cost effective and fast, but suffer from extremely low sensitivity and selectivity due to the similar acoustic properties of healthy cells versus cancerous cells [11]. MRI screening suffers from high prices, long testing time and extremely low specificity, thus only making it useful for women with high breast cancer risk [16]. Finally, CT and PET screening both suffer from being invasive and expensive [11]. Therefore, it is clear that a new screening method is needed that satisfies the primary requirements (cost, time, invasiveness and sensitivity/selectivity).

Many new screening techniques are currently being researched to be used as a primary screening technique. Radar-based microwave imaging, RF based biosensors

and optical biosensors are all potential candidates to become the new screening method, however this report will be discussing the use of piezoelectric biosensors to detect hard tissue buildup (tumours) in soft tissue.

## 1.3 Problem Scope

The piezoelectric effect is defined as the ability for certain materials to create an electrical bias when a mechanical strain is applied [17]. The sensor described in this report uses the piezoelectric effect to measure the difference in deflection that arises when the tactile sensor contacts a soft tissue compared to a hard tissue.

Different designs have already been proposed and implemented to detect a wide variety of cancers (including prostate, breast and skin cancer) [18, 19]. However, the device in this report is based off of the idea that breast cancer cells are far stiffer than those of breast cells. Therefore, if a piezoelectric material with a high response is used, then even small breast tumours that would otherwise be missed by conventional screening methods may be detectable [20]. As described in a paper by Markidou et al., the proposed design would be highly sensitive and selective method that is both non-invasive and fast [2]. The cost of the test would be limited to the cost of device itself and should be generally easy to use, thus the screening would be generally low cost over a large enough populace.

This report builds on the experiments by Markidou et al. by trying Macro Fiber Composites (MFC) as the transducing material instead of lead zirconate titanate (PZT), which was used in the article.

# 2 Design

## 2.1 Reported Design

Currently, there exists a design of piezoelectric cantilevers, also referred to as piezoelectric fingers, towards *in vivo* breast tumour detection. The reported solution is a piezoelectric finger (PEF) acting as a tissue elasticity sensor in a cantilever form with two piezoelectric layers (Figure 1).

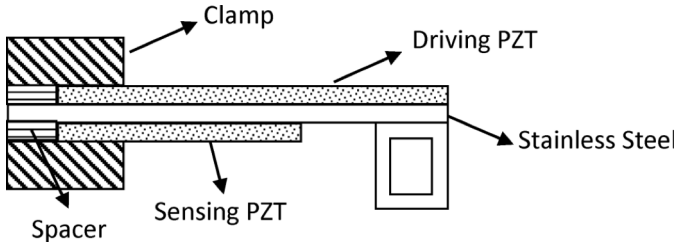


Figure 1: A schematic of a piezoelectric Finger (PEF)[1].

When assembled into an array, these PEFs that can directly measure tissue elastic modulus *in situ* as well as *in vivo* simply by contacting the PEF with the tissue. Applying a direct-current (DC) voltage in the driving piezoelectric layer imparts a force on the tissue by the reverse piezoelectric effect. The corresponding tissue displacement in turn generates an induced voltage in the sensing piezoelectric layer. The tissue elastic moduli can be directly determined from this induced voltage. It has been reported that the induced voltage is proportional to the PEF tip displacement, *d*. Therefore, the induced voltage can be used to deduce the tissue stiffness, E, with the following relationship:

$$E = \frac{1}{2}(\frac{\pi}{A})^{\frac{1}{2}}(1-v^2)\frac{K(V_{in,0}-V_{in})}{V_{in}} \tag{1}$$

where $V_{in,0}$ and $V_{in}$ are the induced voltages without and with the tissue, respectively, $\nu$ is the Poisson's ratio of the tissue, A is the contact area defined by the stainless-steel probe at the tip of the PEF, and K is the effective spring constant of the PEF. The effective spring constant of a designed PEF can be determined through means outlined in previous works [21, 2].

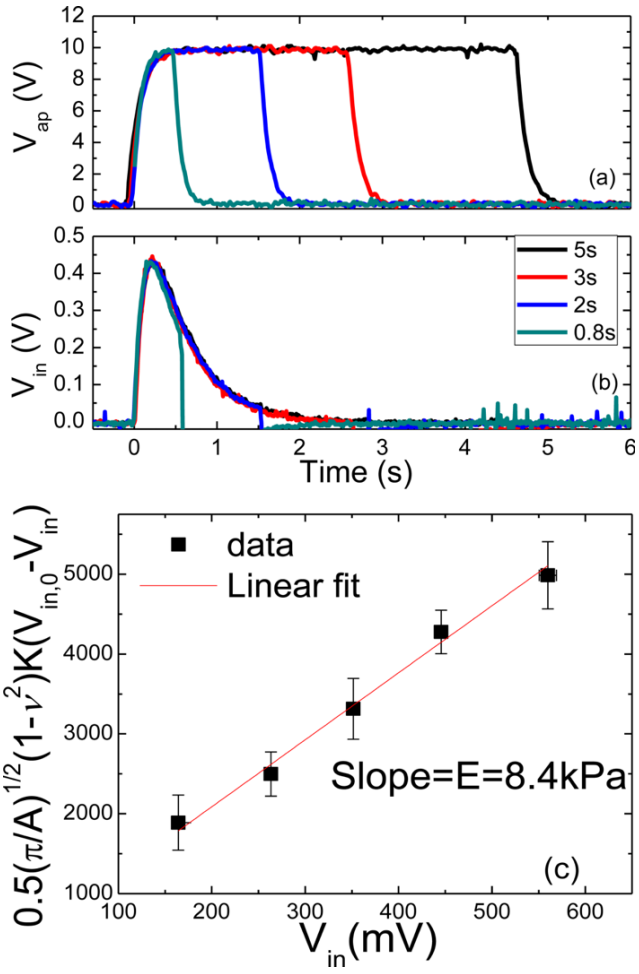


Figure 2: (a) $V_{applied}$ vs. time, (b) $V_{induced}$ vs. time, (c) elastic modulus of module tissue determined with Equation (1) [1].

A lesion is directly detected by contrasting the elastic modulus measured above the lesion with that measured above the surrounding tissues without the need of inversion simulations or pattern recognition software. Normal tissue should generate a elastic modulus measurement of 10kPa while tumours are in the range of 60kPa. The reported solution has been tested on 77 cases of excised breast tissues and demonstrated capable of detecting most types of breast tumours including invasive carcinoma (IC), hyperplasia, brocystic, DCIS, microcalci cations, and even a 3-mm satellite IC missed by mammography and by physician's palpation [1].

A follow-up study was performed to investigate how the DC voltage duration,

the depth at which the hand-held unit is pressed against the breast, and the breast density affects the detection sensitivity. The same reported solution had been developed into a hand-held 4 x 1 PEF array breast tumour detector system towards in vivo patient testing. The tests were carried out at different DC voltage pulses. The detection results showed similar sensitivity, indicating that shortening the duration of the applied voltage did not affect the accuracy of the measurements. It is also shown that for the 15 cases tested for depression depths of 2-6 mm, the detection sensitivity for various tumour sizes were unaffected by different depression depths. Overall, PEF detected 46 of the 48 lesions [1].

## 2.2 Fabrication of a Hand-held Piezoelectric Finger (PEF) Unit

Provided below is a description of the hand-held PEF device fabrication taken directly form the study [1]. The hand-held unit consists of a polycarbonate housing and the 4x1 PEF array. All four PEFs were 6.5 $\pm$ 0.5 mm wide which consists of a 127-$\mu$m thick, 22 $\pm$ 0.5 mm long lead zirconate titanate (PZT) layer at the top for driving, a 50$\mu$m thick, 22 $\pm$ 0.5 mm stainless steel layer in the middle, and a 127$\mu$m thick 12 $\pm$ 0.5 mm PZT layer at the bottom for sensing as schematically shown in Fig. 1 made using a combination of a conductive epoxy and a non-conductive epoxy. A stainless-steel strip was bent into a rectangular loop and glued to the free end of the cantilever (see Fig. 1) using the non-conductive epoxy. The effective spring constant of each individual PEF was used together with Equation (1) to quantify the elastic modulus of tissue measured by that PEF.

## 2.3 PEF Depth Sensitivity

Since the use of PEFs is an indentation technique, it only assesses the mechanical properties of tissues within a certain depth beneath the surface. The depth sensitivity of a PEF is defined as the depth within which the mechanical properties of tissues can be assessed by the PEF. The depth sensitivity of the PEF is determined by its elastic modulus measurements over model tissues containing an array of model tumours of different depths. It is the depth at which the model tumour cannot be distinguished from the surrounding model tissues by elastic modulus measurements. It is reported that regardless of a housing unit, the PEF depth sensitivity is about twice the probe width. By designing a housing that further pushes the probe into

breast tissue, the depth sensitivity can be increased. The same study suggests that a depth sensitivity of at 2 cm is sufficient for regular sized breasts [1]. For larger breasts and deeper tumours, PEFs with a larger probe width can be used. In certain PEF array configurations, measurements have to be performed sequentially to avoid the interference from neighboring PEFs that are activated simultaneously. This may lead to a lengthy scan time when screening for tumours.

## 2.4 Design Adjustments

For the PEF array to be a viable in vivo breast tumour detection tool, it must be able to scan both breasts in a practical amount of time. The most straightforward approach to improving scan time is by increasing the detection tool coverage. There are two methods to achieve a greater coverage area. One approach is to increase the PEF array density, thus allowing more measurements to be taken within an area simultaneously. The other approach is to improve the depth sensitivity of the PEF. Either method may be achieved by employing a piezoelectric material of a higher transduction. By substituting a material with higher transduction, the cantilever component of the PEF requires less displacement to produce an induced voltage. This allows for a smaller cantilever dimensions in the PEF without compromising depth sensitivity of the device. Alternatively, replacing the current piezoelectric layer material with a better transducer may lead to a higher depth sensitivity without having to increase the probe widths, allowing a sparser PEF array configuration. In this configuration, the interference between simultaneous PEF measurements is also minimized.

From a manufacturing perspective, the substitution of PZT as the piezoelectric material of the devices can also significantly reduce the use of harmful substances such as lead (Pb) in the industrial process. One such type of material, suitable for the replacement of PZT, are Macro Fiber Composites (MFC). It has been reported that the material's transverse piezoelectric strain coefficient (d31) is comparable to that of PZT. Furthermore, the higher mechanical flexibility of MFC over PZT makes its especially suitable for PEF operation [4]. This suggests that MFC may make for a superior material for piezoelectric applications.

# 3 Analysis

## 3.1 Mathematical Theory

Based on current research for piezoelectric devices, there appears to be no reported PEF design which incorporates MFCs. Therefore, in order to assess the performance of this design, the electromechanical transduction using monolithic PZT must be compared to that of using MFC. First, a more mathematically thorough understanding of the theory of operation is required. As briefly described in the Design section of this report, applying a voltage to the driving piezoelectric layer imparts a force on the tissue through the induced bending of the cantilever system. The mechanism of operation for this PEF device operates in $d_{31}$ mode, as illustrated in Figure 3.

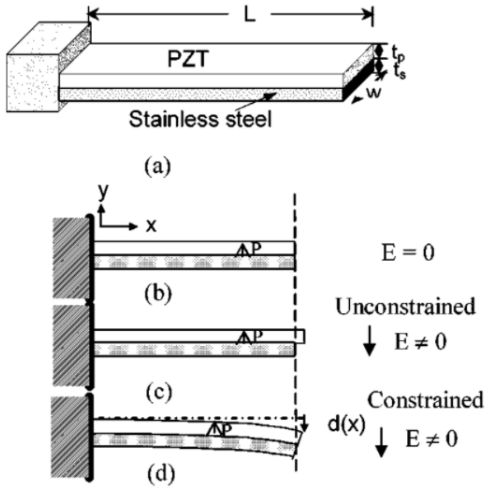


Figure 3: A schematic of the d31 mode of operation for a cantilever comprising of a driving piezoelectric layer (PZT) and a non-piezoelectric layer (Stainless Steel) [2].

The applied electric field causes a lateral strain only in the piezoelectric layer, resulting in a difference in lateral strains between the two layers. Under constrained conditions, this causes the cantilever beam to bend, as depicted in Figure 3(d) [2]. The piezoelectric coefficient, $d_{31}$, relates the electric field applied to the perpendicular strain produced [22]. Thus, a higher $d_{31}$ coefficient should lead to greater electromechanical transduction. There are, however, several trade-offs when determining performance. Typically, monolithic piezoelectric materials such as PZT have high $d_{31}$ coefficients, but are brittle and are thus easily broken at high strains [23].

Therefore, optimization is required in order to assess the trade-offs between flexibility and piezoelectric transduction in a given material. Hereon, when dealing with MFC, only MFC-31 (designed for operation in $d_{31}$ mode) will be considered.

Comparison of the PZT and MFC designs can be achieved by first calculating the bending moment of the cantilever for both cases, by using equation (2).

$$M = (1-\nu)\frac{E_p E_n t_p t_n (t_p + t_n) d_{31} E}{2(E_p t_p + E_n t_n)} \tag{2}$$

In (2), $\nu$ is the Poisson's ratio of the material which the finger is incident on. In this case, the material would be *in situ* breast tissue, which has a reported Poisson's ratio between 0.490-0.499 in literature [24]. $E_n$ is the Young's (tensile) modulus for the non-piezoelectric material, stainless steel, which has a reported value of 180 GPa [25]. Based on the dimensions cited in Xu et al., the thickness of the stainless steel, $t_n$, is 50 $\mu$m. For the monolithic PZT cantilever system, $t_p$ is 127 $\mu$m, and the Young's modulus, $E_p$, for the piezoelectric material, PZT, is 63 GPa [26]. For the MCF cantilever system, the thickness $t_p$ is held constant at 127 $\mu$m, but $E_p$ for MCF is 30.336 GPa [27]. Lastly, PZT has a $d_{31}$ piezoelectric coefficient of 320 pm/V, while the MFC has a $d_{31}$ piezoelectric coefficient of 210 pm/V [22, 28]. Using these numbers, we get the following results:

$$M_{PZT} = 4.82x10^{-3}Nm$$

$$M_{MCF} = 2.01x10^{-3}Nm$$

These results demonstrate that the PZT design is still generating a greater moment than the MFC design, which is expected since the $d_{31}$ piezoelectric coefficient for PZT is larger than that of MFC. This, however, does not necessarily mean that the PZT will outperform the MFC design, since this is only one aspect of the mechanism.

Next, the bending modulus per unit width can be calculated by using equation (3) with the same parameters as outlined above.

$$D = \frac{{E_p}^2 {t_p}^4 + {E_n}^2 {t_n}^4 + 2E_p E_n t_p t_n (2{t_p}^2 + 2{t_n}^2 + 3t_p t_n)}{12(E_p t_p + E_n t_n)} \tag{3}$$

$$D_{PZT} = 4.58x10^{-2}Nm$$

$$D_{MCF} = 2.82x10^{-2}Nm$$

Using these calculated values for M and D for each design, the displacement as a result of voltage-applied bending can be obtained by using equation (4). L, which is defined as the cantilever length, is taken to be 22 mm, while the width, w, is taken to be 6.5 mm [1].

$$d(L) = \frac{ML^2}{2Dw} \tag{4}$$

$$d(L)_{PZT} = 3.92x10^{-3}m$$

$$d(L)_{MCF} = 2.66x10^{-3}m$$

These results demonstrate that the displacement as a result of the induced bending of the cantilever is greater with PZT than with MFC. At first glance, it may appear as though MFC provides no improvement to the existing design. However, the goal of this investigation is to determine whether the MFC design can provide a greater sensitivity in terms of induced voltage in the sensing piezoelectric layer, which is the primary indicator for contrasting the mechanical stiffness of tissues. Therefore, the induced voltage of the cantilever responses must be investigated. Equation (5) demonstrates how induced voltage can be calculated [29].

$$V_{in,ave} = \frac{1}{2}(L_1 + 2L_2)g_{31}\frac{FE_p}{wD}(t_{n1}t_p + \frac{1}{2}{t_p}^2) \tag{5}$$

$L_1$ is the length of the sensing piezoelectric layer (22 mm), whereas $L_2$ is the difference in lengths between the non-piezoelectric layer and the sensing piezoelectric layer (10 mm) [1]. The $g_{31}$ piezoelectric coefficient, similar to the $d_{31}$ coefficient previously described, relates the stress applied (or rather induced by the driving layer in this case) to the open circuit electric field produced [22]. $t_{n1}$ represents the position of the neutral plane, and is given by equation (6).

$$t_{n1} = \frac{E_s{t_s}^2 - E_p{t_p}^2}{2(E_s t_s + E_p t_p)} \tag{6}$$

Since the $g_{31}$ coefficient for the MFC is not well-defined, and the force $F$ is not explicitly applied but rather induced by the driving piezoelectric layer and imparted

onto the steel, the induced voltage cannot be accurately calculated using equation (5). Therefore, COMSOL Multiphysics can be used to simulate the design with both materials, thus allowing for the measurement and comparison of the induced voltages.

## 3.2 COMSOL Simulation

### 3.2.1 General Setup

The PZT-cantilever system was first modeled using the dimensions outlined above. For simplicity, only one PEF was simulated, and it can be assumed that an array would increase the total induced voltage. Fixed constraint boundary conditions (BCs) were applied to the clamped ends of the cantilever layers. The middle non-piezoelectric layer was assigned material properties based on the built-in material for Stainless Steel in COMSOL. The same was done for the top and bottom piezoelectric layers, which were assigned the built-in PZT-5H material. The piezoelectric physics simulation involves the use of a Solid Mechanics module, in combination with an Electrostatics module. For such simulations, the solution can be computed via the Stress-Charge form or the Strain-Charge form, as depicted in Figure (4).

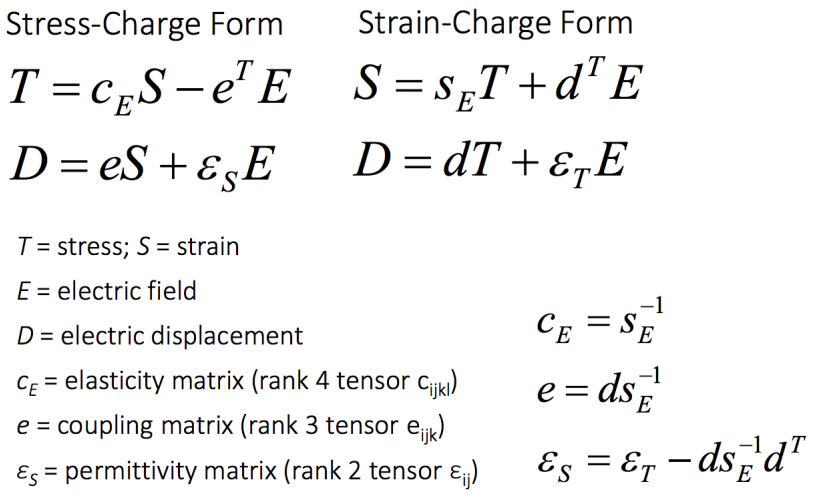


Figure 4: The two methods used by COMSOL for piezoelectric simulation and computation [3].

In order to ensure a correct simulation, the material properties were compared

with those used in the paper for the basis of the design. The PZT-5H properties, found in Table 1, were obtained from a paper by Collet et al., and were found to be accurately corresponding with those built into the COMSOL material [4].

Table 1: Stress-Charge Form Properties for PZT-5H [4].

| | | |
|---|---|---|
| $c_{11}^E = 1.2710^{11}$ Pa | $c_{22}^E = 1.2710^{11}$ Pa | $c_{33}^E = 1.1710^{11}$ Pa |
| $c_{12}^E = 8.0210^{10}$ Pa | $c_{13}^E = 8.4610^{10}$ Pa | $c_{23}^E = 8.4610^{10}$ Pa |
| $c_{44}^E = 2.3010^{10}$ Pa | $c_{55}^E = 2.3010^{10}$ Pa | $c_{66}^E = 2.3410^{10}$ Pa |
| $e_{31} = 6.62$ C/m$^{-2}$ | $e_{33} = -23.24$ C/m$^{-2}$ | $e_{32} = 6.62$ C/m$^{-2}$ |
| $e_{24} = -17.03$ C/m$^{-2}$ | $e_{15} = -17.03$ C/m$^{-2}$ | $\rho = 7500$ kg m $^{-3}$ |
| $\varepsilon_{11}^S = 1704\varepsilon_0$ C V$^{-1}$ m$^{-1}$ | $\varepsilon_{22}^S = 1704\varepsilon_0$ C V$^{-1}$ m$^{-1}$ | $\varepsilon_{33}^S = 143.361\varepsilon_o$ C V$^{-1}$ m$^{-1}$ |

Next, an electric potential was generated by applying two electric potential BCs at the top and bottom of the driving PZT layer, corresponding to the 10 V applied in the paper used for the basis of the design [1]. Floating potential BCs were similarly applied to the top and bottom of the sensing PZT layer, in order to be able to measure the induced voltage.

### 3.2.2 Without Tissue

The PEF cantilever was first simulated without any tissue to observe its performance and obtain a baseline for future comparison. Figure (5) demonstrates the stress field and the displacement field for this "Empty" scenario.

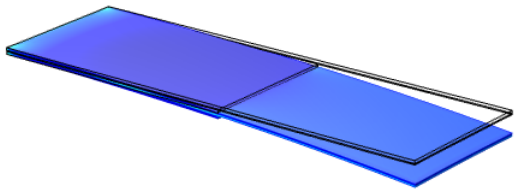

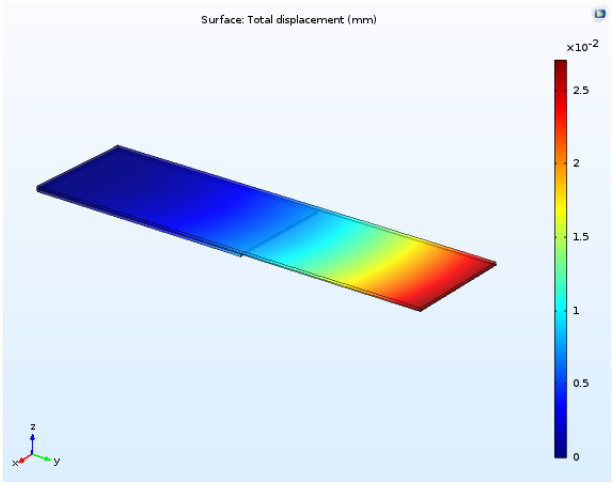


Figure 5: PEF on air a) Stress Field demonstrating cantilever bending. b) Displacement field demonstrating cantilever displacement

### 3.2.3 With Tissue, Without Tumour

To model the breast tissue, the same Poisson's ratio of $\nu = 0.49$ was given, as well as soft tissue density of $1000kg/m^3$, relative permittivity $\epsilon_r = 40$, and a Young's modulus E = 10 kPa [1]. The tissue was modeled as a rectangular block to represent a cross section of the tissue, assuming a flat contact area after depression. The block was made with a greater w than L in order to model an infinite tissue for most accurate local results. Figure (6) demonstrates the stress field and the displacement

field for this "Tissue" scenario.

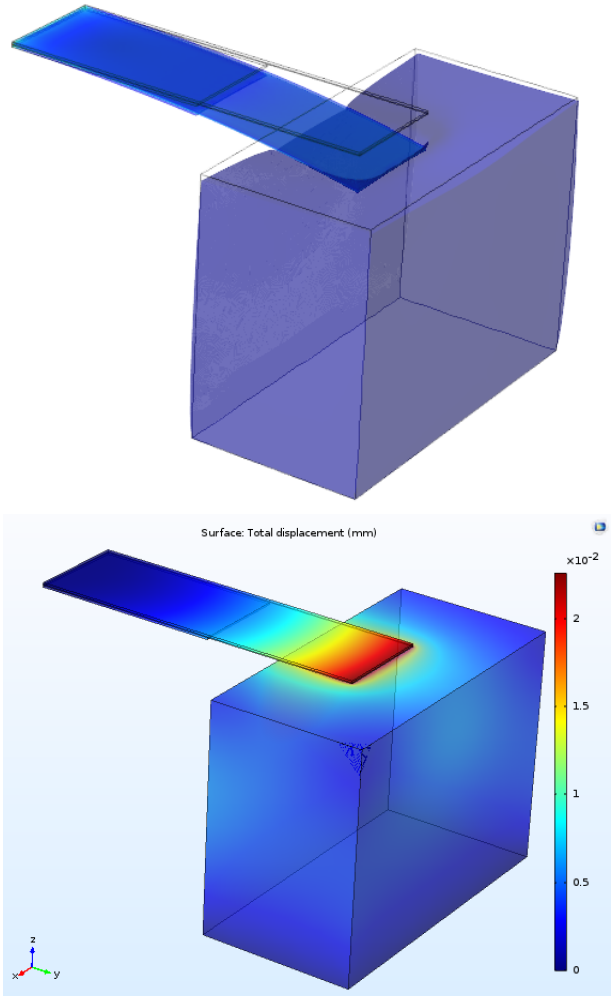


Figure 6: PEF on tissue a) Stress Field demonstrating cantilever bending. b) Displacement field demonstrating cantilever and resulting tissue displacement

### 3.2.4 With Tissue + Tumour

To model the tumour, a 5 mm-diameter sphere was created inside of the tissue, at a depth of 2 mm. This is because the tumour was chosen to be 6 mm deep inside the tissue, and after 4 mm depression of the breast tissue, the tumour would be 2

mm from the surface of the PEF. These numbers were based on the work of Xu et al., and were therefore chosen for consistency [1]. The same tissue parameters were given for the tumour material except for the Young's modulus, which was changed to 60 kPa, as reported by Xu et al. for breast cancer tumours [1]. Again, Figure (7) demonstrates the stress field and the displacement field for this "Tumour" scenario.

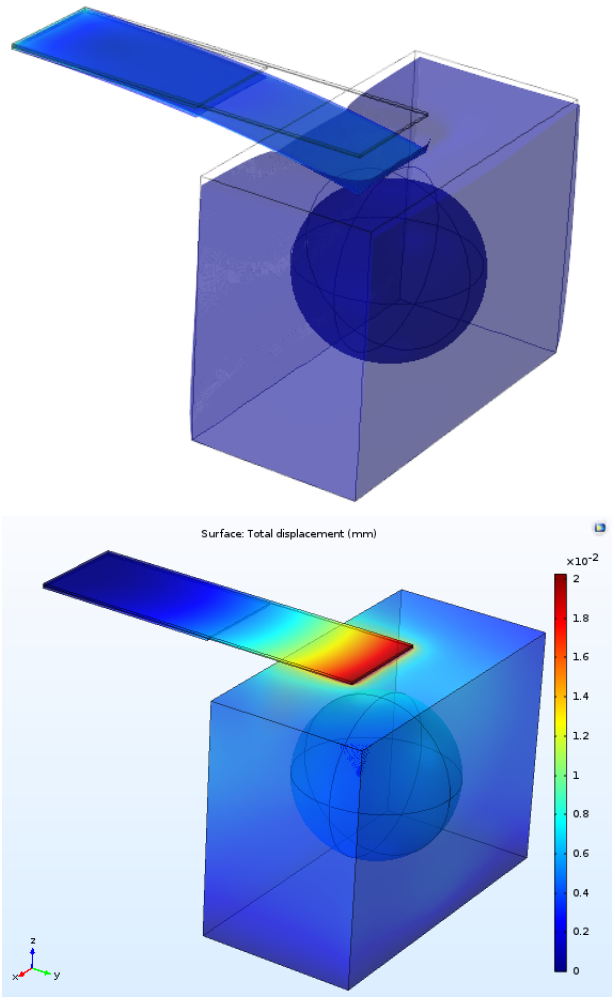


Figure 7: PEF on tissue + tumour a) Stress Field demonstrating cantilever bending. b) Displacement field demonstrating cantilever and resulting tissue displacement

### 3.2.5 Results

All three scenarios were simulated for the PZT material, as well for the MFC material. The MFC properties, found in Table 2, were again obtained from the Collet et al. paper [4], and subsequently input into COMSOL. The results of all of these simulations are found in Table 3.

Table 2: Stress-Charge Form Properties for MFC-31 [4].

| | | |
|---|---|---|
| $c_{11}^E = 3.94 \times 10^{10}$ Pa | $c_{22}^E = 2.03 \times 10^{10}$ Pa | $c_{33}^E = 3.25 \times 10^{10}$ Pa |
| $c_{12}^E = 1.29 \times 10^{10}$ Pa | $c_{13}^E = 0.83 \times 10^{10}$ Pa | $c_{23}^E = 0.53 \times 10^{10}$ Pa |
| $c_{44}^E = 0.55 \times 10^{10}$ Pa | $c_{55}^E = 0.55 \times 10^{10}$ Pa | $c_{66}^E = 1.31 \times 10^{10}$ Pa |
| $e_{31} = -7.12$ C m$^{-2}$ | $e_{33} = 12.1$ C m$^{-2}$ | $e_{32} = -4.53$ C m$^{-2}$ |
| $e_{24} = -17.03$ C m$^{-2}$ | $e_{15} = -17.03$ C m$^{-2}$ | $\rho = 7000$ kg m $^{-3}$ |
| $\varepsilon_{11}^S = 237.2\varepsilon_0$ C V$^{-1}$ m$^{-1}$ | $\varepsilon_{22}^S = 237.2\varepsilon_0$ C V$^{-1}$ m$^{-1}$ | $\varepsilon_{33}^S = 143.4\varepsilon_o$ C V$^{-1}$ m$^{-1}$ |

Table 3: COMSOL Simulation Results for Three Different Scenarios, using either PZT or MFC.

| Material | Structure | Floating Potential (V) | Average Displacement (m) |
|---|---|---|---|
| PZT | Empty | 0.25436 | 0.0270892 |
| PZT | Tissue | 0.11861 | 0.0226025 |
| PZT | Tumour | 0.04646 | 0.020269 |
| MFC | Empty | 0.78747 | 0.0310352 |
| MFC | Tissue | 0.37103 | 0.0184397 |
| MFC | Tumour | 0.2396 | 0.0144965 |

By examining these results, it is clear that the original hypothesis was correct in that MFC can provide a higher sensitivity with regards to detecting tissue stiffness. For each scenario, the MFC material produced a greater induced voltage as compared to the PZT material. Furthermore, the displacement of the PZT-cantilever design was shown to be greater in the tissue and tumour scenarios as compared to the MFC-cantilever, which further supports the conclusions made previously in section 3.1 that a greater displacement does not necessarily mean greater performance. Lastly, the

decreasing floating potential and displacement trends observed make sense, since the presence of a tissue would resist the deformation of the cantilever, and this would be further amplified by the presence of a stiffer material (i.e. tumour) within the tissue.

# 4 Conclusions

Current technologies for detecting breast cancer do not meet all of the primary requirements of an optimal first screening test. For a primary testing method to be deemed optimal, it must be inexpensive, quick, non-invasive and highly selective. This report shows that PEF arrays with MFC layers instead of PZT can potentially meet all these requirements and be used as the next generation of breast cancer screening devices.

The results from the mathematical modeling of the theory behind bimorph cantilever structures (which form the basis of the PEF structure), showed that replacing PZT with MFC in the driving layer would lower the displacement of the bending cantilever. This, however, was hypothesized to not be significant enough to indicate poorer performance in the form of sensitivity (i.e. induced voltage). To prove this, COMSOL was used to simulate both the PZT and MFC designs. Three different scenarios, were constructed for the environment of the device: no tissue, tissue without a tumour, and tissue with a tumour. The results of these simulations not only supported the lower displacement of MFC as compared to PZT, as previously observed, but also demonstrated a higher induced voltage in all three cases despite this. The appearance of a tumour demonstrated a $\sim$0.13 V decrease in induced voltage in the MFC system, as compared to the $\sim$0.07 V decrease in the PZT system. This analysis suggests that MFCs make better transducers than PZT, which is advantageous for PEF array dimensions and depth sensitivity.

Overall, PEF based tactile sensors for breast cancer detection could be relatively inexpensive, could require minimal time to use and could be extremely non-invasive, while also providing high selectivity and sensitivity for breast tumours of many different sizes and depths. Further investigating different cantilever shapes, as well as layer dimensions could help develop the PEF concept into a design for reliable surface detection of tumours and lesions in many different biological tissues. Until then, it is clear that PEF array based devices provide an exciting alternative to the current selection of breast cancer screening methods.

# References


[1] Xin Xu, Youngsoo Chung, Ari D Brooks, Wei-Heng Shih, and Wan Y Shih. Development of array piezoelectric fingers towards in vivo breast tumor detection. *Review of Scientific Instruments*, 87(12):124301, 2016.

[2] Anna Markidou, Wan Y Shih, and Wei-Heng Shih. Soft-materials elastic and shear moduli measurement using piezoelectric cantilevers. *Review of Scientific Instruments*, 76(6):064302, 2005.

[3] COMSOL. Piezoelectric simulations. `https://cdn.comsol.com/wordpress/2014/12/Piezo_COMSOL_50.compressed.pdf`. Accessed: 2018-03-30.

[4] Manuel Collet, Massimo Ruzzene, Ken Cunefare, and Buli Xu. Modeling and characterization of macro-fiber composite transducers for lamb wave excitation. In *Health Monitoring of Structural and Biological Systems 2010*, volume 7650, page 76501H. International Society for Optics and Photonics, 2010.

[5] Mohammad R Mohebian, Hamid R Marateb, Marjan Mansourian, Miguel Angel Mañanas, and Fariborz Mokarian. A hybrid computer-aided-diagnosis system for prediction of breast cancer recurrence (hpbcr) using optimized ensemble learning. *Computational and structural biotechnology journal*, 15:75–85, 2017.

[6] Statistics Canada. Cancer in canada: Focus on lung, colorectal, breast and prostate, 2015. Accessed: 2018-03-30.

[7] American Cancer Society. How common is breast cancer? `https://www.cancer.org/cancer/breast-cancer/about/how-common-is-breast-cancer.html`, 2018. Accessed: 2018-03-30.

[8] Arn Migowski. Early detection of breast cancer and the interpretation of results of survival studies/a deteccao precoce do cancer de mama e a interpretacao dos resultados de estudos de sobrevida. *Ciencia & saude coletiva*, 20(4):1309–1310, 2015.

[9] National Cancer Institute: Cancer Trends Progress Report. Stage at diagnosis. `https://progressreport.cancer.gov/diagnosis/stage`, 2018. Accessed: 2018-03-30.

[10] American Cancer Society. Breast cancer survival rates. `https://www.cancer.org/cancer/breast-cancer/understanding-a-breast-cancer-diagnosis/breast-cancer-survival-rates.html`, 2017. Accessed: 2018-03-30.

[11] Lulu Wang. Early diagnosis of breast cancer. *Sensors*, 17(7):1572, 2017.

[12] Barbro Numan Hellquist, Kamila Czene, Anna Hjälm, Lennarth Nyström, and Håkan Jonsson. Effectiveness of population-based service screening with mammography for women ages 40 to 49 years with a high or low risk of breast cancer: Socioeconomic status, parity, and age at birth of first child. *Cancer*, 121(2):251–258, 2015.

[13] Tracy Onega, L Elizabeth Goldman, Rod L Walker, Diana L Miglioretti, Diana SM Buist, Stephen Taplin, Berta M Geller, Deirdre A Hill, and Rebecca Smith-Bindman. Facility mammography volume in relation to breast cancer screening outcomes. *Journal of medical screening*, 23(1):31–37, 2016.

[14] Douglas G Altman and J Martin Bland. Diagnostic tests. 1: Sensitivity and specificity. *BMJ: British Medical Journal*, 308(6943):1552, 1994.

[15] Charles R Smart. Limitations of the randomized trial for the early detection of cancer. *Cancer*, 79(9):1740–1746, 1997.

[16] Erika J Schneble, Lindsey J Graham, Matthew P Shupe, Frederick L Flynt, Kevin P Banks, Aaron D Kirkpatrick, Aviram Nissan, Leonard Henry, Alexander Stojadinovic, Nathan M Shumway, et al. Future directions for the early detection of recurrent breast cancer. *Journal of Cancer*, 5(4):291, 2014.

[17] What Is. Piezoelectricity. `http://whatis.techtarget.com/definition/piezoelectricity`. Accessed: 2018-03-31.

[18] Xin Xu, Cynthia Gifford-Hollingsworth, Richard Sensenig, Wei-Heng Shih, Wan Y Shih, and Ari D Brooks. Breast tumor detection using piezoelectric fingers: first clinical report. *Journal of the American College of Surgeons*, 216(6):1168–1173, 2013.

[19] Li Su, Lan Zou, Chi-Chun Fong, Wing-Leung Wong, Fan Wei, Kwok-Yin Wong, Rudolf SS Wu, and Mengsu Yang. Detection of cancer biomarkers by piezoelectric biosensor using pzt ceramic resonator as the transducer. *Biosensors and Bioelectronics*, 46:155–161, 2013.

[20] Stewart Sherrit and Binu K Mukherjee. Characterization of piezoelectric materials for transducers. *arXiv preprint arXiv:0711.2657*, 2007.

[21] Hakki Yegingil, Wan Y Shih, and Wei-Heng Shih. All-electrical indentation shear modulus and elastic modulus measurement using a piezoelectric cantilever with a tip. *Journal of Applied Physics*, 101(5):054510, 2007.

[22] PiezoSystems. Psi-5h4e piezoceramic sheets and their properties. `http://www.piezo.com/prodsheet2sq5H.html`. Accessed: 2018-03-30.

[23] Hyun J Song, Young-Tai Choi, Norman M Wereley, and Ashish Purekar. Comparison of monolithic and composite piezoelectric material–based energy harvesting devices. *Journal of intelligent material systems and structures*, 25(14):1825–1837, 2014.

[24] Peter NT Wells and Hai-Dong Liang. Medical ultrasound: imaging of soft tissue strain and elasticity. *Journal of the Royal Society Interface*, 8(64):1521–1549, 2011.

[25] The Engineering Toolbox. Young's modulus - tensile and yield strength for common materials. `https://www.engineeringtoolbox.com/young-modulus-d_417.html`, 2003. Accessed: 2018-03-30.

[26] MEMnet. Material: Lead zirconate titanate (pzt). `https://www.memsnet.org/material/leadzirconatetitanatepzt/`. Accessed: 2018-03-30.

[27] Smart Material. Mfc engineering properties. `https://www.smart-material.com/MFC-product-properties.html`, 2018. Accessed: 2018-03-30.

[28] SmartMaterial. Macro fiber composite - mfc. `https://www.smart-material.com/media/Datasheets/MFC_V2.3-Web-full-brochure.pdf`. Accessed: 2018-03-30.

[29] Xiaotong Gao, Wei-Heng Shih, and Wan Y Shih. Induced voltage of piezoelectric unimorph cantilevers of different nonpiezoelectric/piezoelectric length ratios. *Smart Materials and Structures*, 18(12):125018, 2009.